Characteristic, Structure, and Morphology of Carbon Deposit From Biodiesel Blend

J.A. Hidayat
Graduate School of Mechanical Engineering Universitas Indonesia

Sugiarto, Bambang
Faculty of Engineering, Universitas Indonesia

https://doi.org/10.5109/4150514

出版情報：Evergreen. 7 (4), pp.609-614, 2020-12. 九州大学グリーンテクノロジー研究教育センター
バージョン：

Characteristic, Structure, and Morphology of Carbon Deposit From Biodiesel Blend

J.A. Hidayat[1], Bambang Sugiarto[2*]

[1]Graduate School of Mechanical Engineering Universitas Indonesia, Depok 16424 Indonesia

[2]Faculty of Engineering, Universitas Indonesia, Depok 16424 Indonesia

*Corresponding Author's email: bangsugi@eng.ui.ac.id

(Received November 4, 2020; Revised December 9, 2020; accepted December 16, 2020).

Abstract: The occurrence of deposits in the combustion chamber greatly affects engine performance and can affect engine emissions. This will continue to happen when using fuels derived from fossil fuels. To determine the occurrence of these deposits, research is carried out to determine the process of deposit formation, composition and structure as well as other influences that can cause deposits to occur to overcome deposits in the engine room. The purpose of this study was to determine the structure, morphology of Biodiesel B30 deposit Fatty Acid Methyl Esters (FAME), and Hydrotreated B30 from deposition test rigs using Scanning Electron Microscopy (SEM) and EDX (Energy Dispersive X-Ray) methods. Based on this test, the carbon element in the Biodiesel B30 FAME deposit is higher than that of hydrotreated fuel. Other components are also found in B30 FAME such as Oxygen, Nitrogen and also found in metal elements, which in Hydrotreated only a little

Keywords: deposits in the combustion chamber; scanning electron microscopy ; hydrotreated B30; deposit formation; deposition test rig; structure deposit of biodiesel

1. Introduction and background

The use of fossil fuels as diesel fuel causes a rapid reduction in fossil fuels. This encourages researchers to develop or look for alternative fuels that can replace or limit the use of fossil fuels. Biodiesel is an option that can be used as an alternative fuel[1)]. Many studies with various variations of biodiesel and various methods applied to the engine[2-4)]. Jena et al. In his research using the types of petro diesel (PD) and palm biodiesel (PB), it shows that the performance of machines using biodiesel derived from oil palm is better than using karanja[5)].

The use of biodiesel as an alternative fuel, still causes problems, including deposits of combustion results in the combustion chamber. One of the products produced from the fuel combustion process is carbon, a collection of hard black and black soot on engine parts such as cylinder heads, cylinder walls, pistons, and valves, which can therefore, It will affect engine performance, tribology properties, so that it will cause a lot of oil consumption, and high temperature in the engine. A number of studies have focused on deposits originating from conventional fuels and alternative fuels, although not many.

Uy et al. reported the nanostructures of gasoline fuel deposits, and compared major deposit particles from exhaust gases and from engine oil[6)]. Bambang Sugiarto et al. in his research to obtain the characteristics the formation of deposits in the combustion chamber where the B20 biodiesel sample is mixed with essential oil with a ratio of 1: 2000,1: 3000,1: 4000 and 1: 5000[7)]. Baker et al. in his research Effect of Fuel Additives on the composition and formation of deposits by spectroscopic analysis [8)]. Gregory et al. Has been reported in his research that the influence of unburned fuel, exhaust gas contaminants as well as engine oil on the formation and formation of deposits[9)].

In a study of 512 hours endurance test using 40% castor oil biodiesel and diesel oil, it is said that dry deposits are found in biodiesel rather than oily diesel deposits[10)]. B100 biodiesel palm oil experiments for 800 hours have been carried out using Kubota diesel engine 14 HP and showed deposits on the cylinder head, piston crown, and injector[11)]. Wander et.al in his research showed deposits on diesel are lower than pure soybean esters (SME 100)[12)]. In another study using the hot surface method/HSDT, which showed that hot surface temperatures located near the MEP temperature have the potential to reduce the formation of deposits on hot surfaces[13)]. Yanmar L48 diesel was used in a 200-hour endurance test using B50 biodiesel, wet and brittle sediment was found on the engine piston surface after the endurance test[14)]. KOME 20 biodiesel fuel and diesel The endurance test method for 250 hours shows that the deposit on the KOME 20 fuel injector tip is more than the diesel fuel injector[15)].

Several studies have also been carried out to classify the structure of deposits from fuel[16-19)]. Various methods were carried out to find out the elements in the deposit, including electron microscopy, solid-state C resonance nuclear, FTIR, gas chromatography-mass spectrometry, and other techniques, and the elements being analyzed including Oxygen Carbon, Potassium and others[20-22].

Hoang et al. **i**n his research observing an increase in the number of deposits that occurred in injector tips with DF, SJO30 and PSJO90 fuels using SEM[23]. Liquat et al. in his study used SEM and EDS to identify carbon deposits in PB 20 and Diesel Fuel and found a larger deposit in PB 20 compared to Diesel Fuel[24]. Celik et al. by using B100 fuel and diesel fuel in the engine after running for 200 hours. And reported a significant increase in the number of elements in the B100 structure[25].
The purpose of this research is to conduct a comparative study of the composition or structure of the biodiesel deposit with a mixture of FAME and HVO as a consideration for further research in order to remove deposits in the combustion chamber when using biodiesel fuel.

2. Method and experimental setup

In this study, the fuel used as a sample was fuel from Pertamina B30 (30% biodiesel,70% Diesel Fuel by volume) FAME SNI (Indonesian national standard) and HVO (hydrotreated Vegetable Oil) diesel fuel. Fatty Acid Methyl Ester (FAME) is an alternative fuel for diesel engines derived from the transesterification process of plant oils or animal fats with the addition of methanol[26]. Hydrotreated Vegetable Oil (HVO) has become biodiesel obtained from the hydrotreating process. In the HVO production process, hydrogen is used to remove oxygen from triglycerides (vegetable oils)[27]. This test was carried out by dropping the fuel droplets on the hot plate inside the Furnace (figure 2) from the fuel tank through the needle with the room temperature assumed to be in accordance with the engine combustion chamber because the temperature of the diesel engine combustion chamber can vary as needed. The hot plate used is from AISI 304, with dimensions of Length 100 mm, Width of 100 mm and 0.8 mm thick. Table 1 shows the parts of the Furnace (Hot chamber test rig)[28]. In this study, the structure, morphology of the biodiesel carbon deposit was studied experimentally.

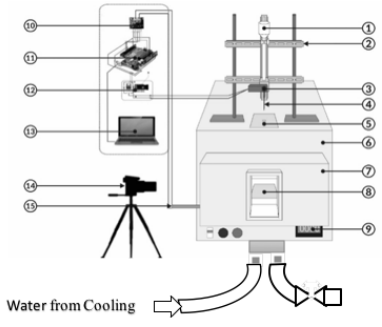

Fig. 1: Hot Chamber Deposition Test Rig

Table 1. The Caption of Hot Room Temperature Test Rig

1	Fuel tank
2	Buffer fuel container
3	Solenoid valve Shako PU220AR02-24V
4	Needle
5	The droplet entry holes into the furnace
6	Furnace with heater capacity up to 1200°C
7	Furnace door
8	Hot plate (AISI 304)
9	Furnace temperatur control
10	K type thermocople module (Max 6675)
11	Arduino UNO R3 microcontroller
12	Power supply 24 VDC & relay solenoid
13	Laptop, temperatur data display
14	Video camera
15	K type thermocouple

In the process of testing the fuel to obtain the amount of mass of the deposit, the plate was put into a hot chamber, then waited about 10 seconds to ensure that the temperature of the hot plate is the same as the room temperature the fuel being tested was dropped continuously on a hot plate at three-second intervals with the temperature set according to need. At each temperature, fuel is dropped up to 10.000 times, then every 2.000 drops a mass deposit is measured.
Fuel density and viscosity measurements were carried out using the Anton Paar SVM 3000 Stabinger Viscometer. Mass measurements were carried out with a digital analytical scale (ADAM PW 254). While the structure of the sediment was examined through Scanning Electron Microscopy (SEM). The test was conducted at the Laboratory of the Department of Metallurgy and Materials Engineering (DTMM), Faculty of Engineering, University of Indonesia using a SEM microscope Inspect F50.

3. Results and Discussion

3.1 Mass Deposit

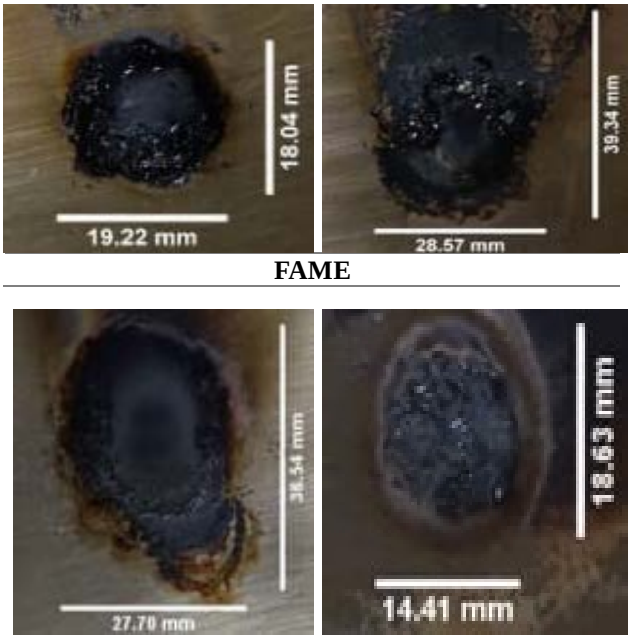

Fig. 2: Photographic View of Deposit

As shown in Fig. 2, deposit the test results with the test rig method photographed during the test with temperatures of 250 ºC in left side and 350 ºC in right side on FAME and HVO fuels. Visual inspection after testing up to 10,000 drops reveals some accumulation of different deposits and surfaces. In fig. 2 shows the fame fuel has a rougher and thicker surface compared to HVO.

3.2 Scanning Electron microscopy (SEM) and Energy Dispersive Spectroscopy

SEM (scanning electron microscopy) are used to observe microstructure, and zones are chosen to analyze elemental content[29-32]. Fig. 3-6 letter A shows a micro image of the surface of the Fame deposit at a temperature of 250ºC and 350 ºC after testing using the deposition test rig method with 10,000 droplets. EDS is used to obtain the element content in carbon deposits to further know the process of deposition. Fig. 3-6 letter A-B, show the EDS analysis area of the deposit.

Fig. 3 shows an enlarged SEM image of the FAME B 30 deposit at 250 ºC. Fig. 3A-B shows the analysis of EDS elements at others position (A-B) on the deposited surface shown in Fig. 3. It can be seen that the deposits are relatively thick and overlapping. All deposited layer locations indicated by the A-B location were dominated by carbon and oxygen, with the following amount in percentage of mass: 57.35% at point A and 56% at point B for the element Carbon, while for the element Oxygen respectively 36.71% and 37. 31%.

A

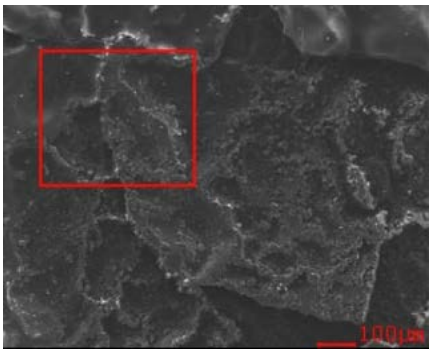

Element	Wr%	Ar%
CK	57,35	64,73
NK	3,80	03,68
OK	36,71	31,11
SiK	00,33	00,16
MoL	01,25	00,18
SK	00,05	00,02
CrK	00,14	00,04
FeK	00,26	00,06
NiK	00,10	00,02

B

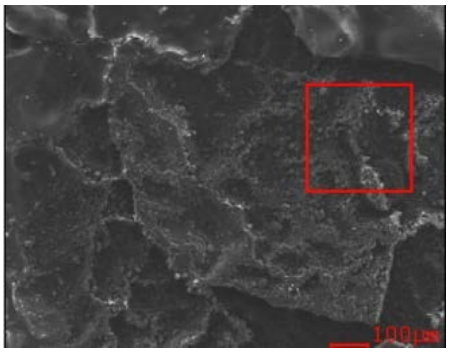

Element	Wr%	Ar%
CK	56,00	63,63
NK	04,03	03,92
OK	37,31	31,83
SiK	00,40	00,20
MoL	01,26	00,18
SK	00,00	00,00
CrK	00,35	00,09
FeK	00,44	00,11
NiK	00,19	00,05

Fig. 3: FAME at Temperature 250ºC.

Nitrogen is found at each point by 3.80% and 4.03%. While other elements are only a few such as Fe, Ni, Cr, Si, S. it shows that few metal elements were found in the B30 FAME diesel fuel.

Fig. 4 shows an enlarged SEM image of the FAME B 30 deposit at 250 ºC. Fig. 4A-B shows the analysis of EDS elements at different locations (location A-B) on the deposited surface shown in Fig. 3a. It can be seen that the deposits are relatively thick and overlapping. All deposited layer locations indicated by the A-B location were dominated by carbon and oxygen, with the following amount in percentage of mass: 54.03% at position A, 50% at position B. However, oxygen concentration at this location was found as: 26.85% at location A, 20.29% at location B, respectively. Apart from that, the discovery of other elements that could not be identified, among others nitrogen (N) and silicon (Si), sulfur (S). There was a decrease in the mass of carbon and oxygen at FAME at 350 ºC compared to 250 ºC.

Fig. 5 shows an enlarged SEM image of the HVO B 30 deposit at 250 ºC. Fig. 5A-B shows the analysis of EDS elements at different locations (location A-B) on the deposited surface shown in Fig. 5 It can be seen that the deposits are relatively thick and overlapping. All deposited layer locations indicated by the A-B location were dominated by carbon and oxygen, with the following amount in percentage of mass: 60.11% at location A, 60.89% at location B. However, the oxygen level at this

position was found as 30.85% at position A 29.55% at location B, respectively. Nitrogen is found at each point by 4.04% and 2.51 %. While other elements are only a few such as Fe, Ni, Cr, Si, S. it shows that few metal elements were found in the B30 HVO diesel fuel at temperature 250 ºC. Apart from that, the discovery of other elements that could not be identified, among others nitrogen (N) and silicon (Si). Whereas the HVO B30 fuel with a temperature of 350 ºC at all deposited layer locations indicated by location A-B in Fig.6 shows a higher carbon concentration. In this case, carbon concentrations at these position were obtain 58,38% at position A, 48,95% at position B.

A

Element	Wr%	Ar%
CK	54,03	66,85
NK	03,80	04,03
OK	26,85	24,94
SiK	00,64	00,34
MoL	01,83	00,28
SK	00,48	00,22
CrK	02,95	00,84
FeK	07,96	02,12
NiK	01,47	00,37

B

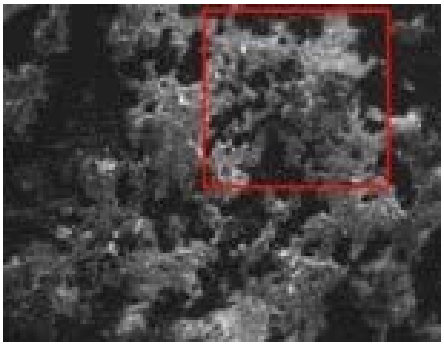

Element	Wr%	Ar%
CK	50,01	67,95
NK	03,02	03,52
OK	20,29	20,70
SiK	00,50	00,29
MoL	01,86	00,32
SK	00,22	00,11
CrK	04,92	01,54
FeK	16,50	04,82
NiK	02,68	00,74

Fig. 4: FAME at Temperature 350 ºC.

A

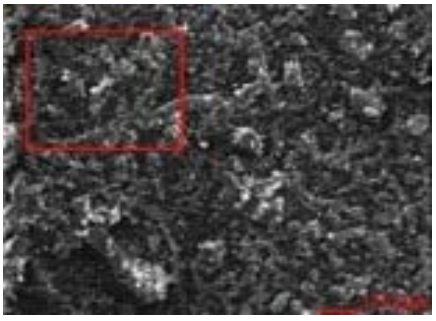

Element	Wr%	Ar%
CK	60,11	68,24
NK	04,04	03,93
OK	30,85	26,29
SiK	00,51	00,25
MoL	01,02	00,15
SK	01,62	00,69
CrK	00,18	00,05
FeK	01,68	00,41
NiK	00,00	00,00

B

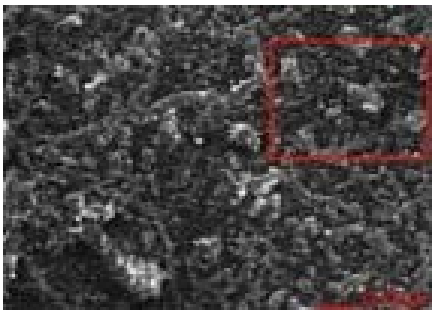

Element	Wr%	Ar%
CK	60,89	70,13
NK	02,51	02,48
OK	29,55	25,55
SiK	00,31	00,15
MoL	02,09	00,30
SK	01,20	00,52
CrK	00,63	00,17
FeK	02,35	00,58
NiK	00,47	00,11

Fig. 5: HVO at Temperature 250 ºC.

However, oxygen concentrations at this location were found as 38,97% at location A, 44,29% at location B, respectively. It should be noted that some metal elements were found in deposition of diesel-fueled engines while not at HVO B30 at temperatures 350º.

A

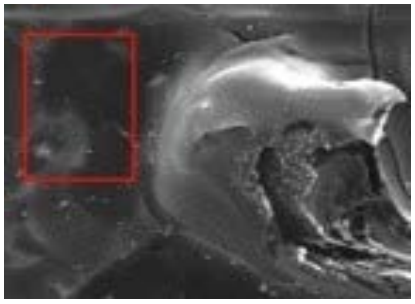

Element	Wr%	Ar%
CK	58,38	65,09
NK	02,20	02,10
OK	38,97	32,62
SiK	00,45	00,19

B

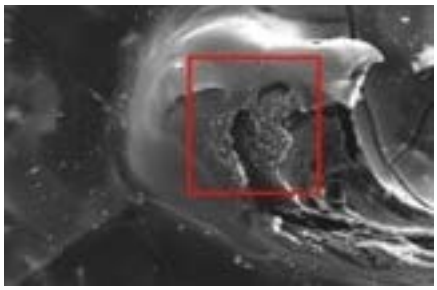

Element	Wr%	Ar%
CK	48,95	55,68
NK	06,58	06,42
OK	44,29	37,83
SiK	00,18	00,08

Fig. 6 : HVO at Temperature 350 ºC

3. Conclusions

In this study, the influence of Biodiesel FAME and HVO as base fuel and B30 mixture in the Hot Chamber Test Rig testing process, with variations in temperatures of 250 ºC and 350 ºC was investigated. Based on the results of the experiment, SEM and EDS analysis on the Hot Chamber Test Rig test shows that the mass of the deposit at B30 HVO is less than the fuel using B30 FAME. Element C in the deposit of B30 HVO fuel is generally higher than that of B30 FAME, while the O content in the deposit of B 30 FAME is lower than that of B30 HVO. In the B30 HVO almost no metal element was found as in the B30. Temperature greatly affects the structure of the deposit of each type of HVO and FAME fuel.

The deposit structure in FAME is black with white spots rough, and dry spots, while HVO tends to be wet, smooth and not porous.

References

1) Pehan, S., et al., "Biodiesel influence on tribology characteristics of a diesel engine". *Fuel*, 2009. **88**(6): p. 970-979.
2) Macor, A., F. Avella, and D. Faedo, "Effects of 30% v/v biodiesel/diesel fuel blend on regulated and unregulated pollutant emissions from diesel engines". *Applied Energy*, 2011. **88**(12): p. 4989-5001.
3) Suryantoro, M.T., et al.,"Effect of temperature to diesel (B0) and biodiesel (B100) fuel deposits forming". *AIP Conference Proceedings*, 2019. **2062**(1): p. 020044.
4) Imam Paryanto et al., "The effect of outdoor temperature conditions and monoglyceride content on the precipitate formation of Biodiesel blended fuel (BXX)". *Evergreen*. **2019. 6** (1), pp.59-64
5) Jena, J. and R.D. Misra, "Effect of fuel oxygen on the energetic and exergetic efficiency of a compression ignition engine fuelled separately with palm and karanja biodisels". *Energy*, 2014. **68**: p. 411-419.
6) Uy, D., et al., "Characterization of gasoline soot and comparison to diesel soot: Morphology, chemistry, and wear". *Tribology international*. **80**: p. 198-209.
7) Suryantoro, M.T., et al., "Biodiesel deposit characterization on hot chamber test rig with biodiesel fuels (B20) and bioaditif essential oil (atsiri)". *E3S Web of Conferences*, 2018. **67**: p. 2016.
8) Barker, J., et al., "Spectroscopic Studies of Internal Injector Deposits (IDID) Resulting from the Use of Non-Commercial Low Molecular Weight Polyisobutylenesuccinimide (PIBSI)". *SAE Int. J. Fuels Lubr*., 2014. **7**(3): p. 762-770.
9) Guinther, G., G. Gregory, and S. Scott, "Formation of Intake Valve Deposits in Gasoline Direct Injection Engines". *SAE International journal of fuels and lubricants*. **9**(3): p. 558-566.
10) Kumar, N., Varun, and S.R. Chauhan, "Evaluation of endurance characteristics for a modified diesel engine runs on jatropha biodiesel". *Applied Energy*, 2015.

155: p. 253-269.
11) Suthisripok, T. and P. Semsamran, "The impact of biodiesel B100 on a small agricultural diesel engine". *Tribology International*, 2018. **128**: p. 397-409.
12) Wander, P.R., et al., "Durability studies of mono-cylinder compression ignition engines operating with diesel, soy and castor oil methyl esters". *Energy*, 2011. **36**(6): p. 3917-3923.
13) Mohamed Arifin, Y. and M. Arai, "Deposition characteristics of diesel and bio-diesel fuels". *Fuel*, 2009. **88**(11): p. 2163-2170.
14) Suryantoro, M.T., B. Sugiarto, and F. Mulyadi, "Growth and characterization of deposits in the combustion chamber of a diesel engine fueled with B50 and Indonesian biodiesel fuel (IBF)". *Biofuel Research Journal*, 2016. **3**(4): p. 521-527.
15) Dhar, A. and A.K. Agarwal, "Effect of Karanja biodiesel blend on engine wear in a diesel engine". *Fuel*, 2014. **134**: p. 81-89.
16) Zerda, T.W., et al., "Surface area, pore size distribution and microstructure of combustion engine deposits". *Carbon*, 1999. **37**(12): p. 1999-2009.
17) Zhang, X., et al., "Investigating the microstructures of piston carbon deposits in a large-scale marine diesel engine using synchrotron X-ray microtomography". *Fuel*, 2015. **142**: p. 173-179.
18) Zerda, T.W., X. Yuan, and S.M. Moore, "Effects of fuel additives on the microstructure of combustion engine deposits". *Carbon (New York)*, 2001. **39**(10): p. 1589-1597.
19) Wang, X., et al., "Effect of lubricant oil additive on size distribution, morphology, and nanostructure of diesel particulate matter". *Applied energy*. **130**: p. 33-40.
20) Feld, H. and N. Oberender, "Characterization of Damaging Biodiesel Deposits and Biodiesel Samples by Infrared Spectroscopy (ATR-FTIR) and Mass Spectrometry (TOF-SIMS)". *SAE International Journal of Fuels and Lubricants*, 2016. **9**(3): p. 717-724.
21) Patel, M., et al., "Morphology, structure and chemistry of extracted diesel soot -- Part I: Transmission electron microscopy, Raman spectroscopy, X-ray photoelectron spectroscopy and synchrotron X-ray diffraction study". *Tribology international*. **52**: p. 29-39.
22) Xu, Y., et al., "Comparison and Analysis of the Influence of Test Conditions on the Tribological Properties of Emulsified Bio-Oil". *Tribology Letters*, 2014. **55**(3): p. 543-552.
23) Hoang, A.T., A.T. Le, and V.V. Pham, "A core correlation of spray characteristics, deposit formation, and combustion of a high-speed diesel engine fueled with Jatropha oil and diesel fuel". *Fuel*, 2019. **244**: p. 159-175.
24) Liaquat, A.M., et al., "Impact of palm biodiesel blend on injector deposit formation". *Applied Energy*, 2013. **111**: p. 882-893.
25) Celik, I. and O. Aydin, "Effects of B100 Biodiesel on Injector and Pump Piston". *Tribology Transactions*, 2011. **54**(3): p. 424-431.
26) Cunshan, Z., et al., "Opportunities and challenges for biodiesel fuel". *Applied energy*, 2011. **88**(4): p. 1020-1031.
27) Arvidsson, R., et al.," Life cycle assessment of hydrotreated vegetable oil from rape, oil palm and Jatropha". *Journal of Cleaner Production*, 2011. **19**(2): p. 129-137.
28) Sugiarto, B., et al., "The effect of antioxidant additives on the growth of deposits on the use of biodiesel fuel (B100) at certain temperatures". *IOP Conference Series: Earth and Environmental Science*, 2018. **105**: p. 12075.
29) S. Harini, et al., "Tensile Properties of Kenaf?E-glass Reinforce hybrid Polypropylene (PP) composites with different fiber loading". *Evergreen*: 2018. **5. (02)** : p. 1-5.
30) Wulan P., et al., "The effect of nickel coating on stainless steel 316 on growth of carbon nanotube from polypropylene waste". *Evergreen*: 2019. **06. (01)** : p. 98-102.
31) Raharjo W.P. et al., "Characterization of sodium bicarbonate treated zalacca fibers as composite reinforcements". *Evergreen*: 2019. **06. (01)** : p. 29-38.
32) Hashizaji K. et al., "Charge-discharge characteristics of Li/$CuCl_2$ Batteris with LiPF6/Methyl difluoroacetate electrolyte". *Evergreen*: 2019. **06. (01)** : p. 01-08.